First-principles calculations of oxygen-vacancy dipoles and hydrogen impurities in SrF_2

R. Jia,* H. Shi,† and G. Borstel
Fachbereich Physik, Universität Osnabrück, D-49069 Osnabrück, Germany
(Received 15 July 2008; published 3 December 2008)

The electronic and atomic properties of oxygen-vacancy dipoles and hydrogen impurities, which are important types of point impurities in the alkaline-earth fluoride SrF_2, are calculated. The band gap of SrF_2 for four different arrangements of O_V dipoles is found at 11.3 eV when calculated with the hybrid B3PW (which is Becke's exchange functionals using Becke's three-parameter method combined with the nonlocal correlation functional of Perdew and Wang) method and is essentially the same as in the perfect SrF_2 crystal. On the basis of the calculated density of states the nature of the defect bands in the band structure can be well understood. In addition two kinds of hydrogen impurities (H_s^-,H_i^0) are also calculated with the B3PW method. We present the corresponding electronic structure and calculate the hyperfine constants at the H_i^0 impurity, which exhibits an unpaired electron, and at its nearest-neighbor fluorine atoms. Our results agree well with the experimental data.

DOI: 10.1103/PhysRevB.78.224101 PACS number(s): 71.15.Mb, 71.20.Dg

I. INTRODUCTION

SrF_2 is a large gap fluoride with $Fm3m$ structure similar to other alkaline-earth fluorides (CaF_2, BaF_2). The cation Sr^{2+} locates at the origin point in the three-atom face-centered-cubic unit cell and two anions F^- on the diagonal points $(\frac{1}{4}a,\frac{1}{4}a,\frac{1}{4}a)$ and $(\frac{3}{4}a,\frac{3}{4}a,\frac{3}{4}a)$, where a is the lattice constant (a=5.799 Å in experiment).[1] In recent years several experimental and theoretical investigations[2–6] of SrF_2 have been performed. Two basic point impurities (oxygen-vacancy dipole and hydrogen impurity) have been identified and studied. For oxygen-vacancy dipoles there exist four different possible arrangements.

For hydrogen impurities there exist two kinds: the first one is the case that the hydrogen atom substitutes a fluorine atom in the system, we call it H_s^- impurity. In this system the number of electrons is still even and all electrons are spin paired. The corresponding defect band consists of s orbitals from the hydrogen atom. In the second case, we call it H_i^0 impurity, the hydrogen atom does not substitute any atom but occupies the center position in the unit cell, which in turn results in an odd number of electrons and thus in the occurrence of an unpaired electron. Due to this unpaired electron the spin polarization around this hydrogen atom is very large, but the effect on the other atoms is only weak. Since the exchange interaction operates only for electrons with parallel spin and the number of electrons is odd, the energy level of the defect band, which consists of s orbitals of the hydrogen atom, now becomes spin split. We call the defect band with lower-energy level α band and with higher-energy level β band. But according to the spin selection rules we know that the electron has no chance to be excited from α band to β band.

We calculate the hyperfine constants at the inserted hydrogen atom and at its nearest neighbors (eight fluorine atoms) at the end of this work. In experiments, the isotropic and anisotropic hyperfine constants are denoted by a and b. According to Weil *et al.*,[7] we calculate these two hyperfine coupling constants (in the units of MHz) by

$$a = \frac{A_0}{h}10^{-6} = \frac{2\mu_0}{3h} g\beta_e g_n \beta_n |\psi_{\alpha-\beta}(0)|^2 10^{-6}, \tag{1}$$

$$b = \frac{\mu_0}{4\pi h} g\beta_e g_n \beta_n \left[T_{11} - \frac{1}{2}(T_{22}+T_{33}) \right], \tag{2}$$

where $|\psi_{\alpha-\beta}(0)|^2$ is the spin density at the origin. The factor g_n of different nuclei can be found in Refs. 7 and 8. For simplification, here we used the factor g of a free electron instead of the factor of the interacting electron g_e. h is the Planck constant, μ_0 is the permeability in vacuum, and β_e and β_n are the electron and nuclear magnetons, respectively. The elements of the tensor **T** are obtained from the gradient of the spin density.

The formation energies of the O_V dipole impurities in an n-atom supercell can be expressed as

$$E_f = E_d^{n-1} + 2E_F - E_O - E_p^n, \tag{3}$$

where E_F and E_O denote the total energy of a single fluorine and oxygen atoms, and E_d^{n-1} and E_p^n the total energies of the crystal with and without an O_V dipole impurity, respectively. In a similar definition we used the following equations to calculate the formation energies of H_s^- and H_i^0 impurities in the crystal:

$$E_f(H_s^-) = E_d^n + E_F - E_H - E_p^n, \tag{4}$$

$$E_f(H_i^0) = E_d^{n+1} - E_H - E_p^n, \tag{5}$$

where E_H denotes the total energy of a single hydrogen atom.

II. METHODOLOGY AND PARAMETERS OF CALCULATIONS

The 2006 version of the CRYSTAL computer code, i.e., CRYSTAL06, is used in this work to calculate the electronic and optical properties of SrF_2 with oxygen-vacancy dipoles and hydrogen impurities. As in our former work,[13–16] we implemented in our calculations the hybrid method: Becke's exchange functionals using Becke's three-parameter method[9] is combined with the nonlocal correlation functional of Perdew and Wang (B3PW).[10–12]

CRYSTAL06 can calculate periodic systems by using the

TABLE I. Formation of energies of four different O_V dipole arrangements and two hydrogen atom impurities in a 96-atom supercell with B3PW method by using Eqs. (3)–(5) in units of eV.

	$O_V\langle 100\rangle$	$O_V\langle 110\rangle$	$O_V\langle 111\rangle a$	$O_V\langle 111\rangle b$	H_s^-	H_i^0
E_f	168.95	169.21	169.32	169.15	12.40	0.07

approximation of linear combination of atomic orbitals (LCAO).[17,18] The basis set of Sr we used in our work was from Habas[19] and supplemented by the Hay-Wadt small-core effective core pseudopotential (ECP). The F-basis set was from Nada.[20] For the impurities the basis set of the oxygen atom was from Valenzano,[21] and as the basis set of the vacancy we use a very simple basis set from Mallia.[22] We have shown in our former work that this quite simple basis set, we named this set 1_s(0.073), gives a more accurate physical description in alkaline-earth fluoride systems than other kinds of basis sets for the vacancies. It also saves computational costs. In the simulations of the SrF_2 crystal with hydrogen impurities we use the result from Dovesi[23] as the basis set of the hydrogen atom.

The reciprocal space integration is performed by sampling the Brillouin zone of the unit cell with the $8\times8\times8$ Pack-Monkhorst net.[24] All defect calculations reported here take the relaxation of the neighboring atoms toward their new equilibrium positions into account. We calculated the formation energies of each defect as a function of supercell size. The results prove the same as shown in Refs. 13–16 that the formation energies are converged already in the 48-atom supercell case. The present calculations for O_V dipoles and hydrogen impurities are all done with 96-atom supercells, which thus is sufficient to guarantee converged results. The corresponding results for the formation energies of the defects are presented in Table I. For the lattice constant of SrF_2 crystal we use the value (5.845 Å) from our former work.[16] The direct band gap of the perfect SrF_2 bulk (11.31 eV) was already calculated in that work.[16] The effective charges of atoms and overlap populations between nearest neighbors are obtained using the standard Mulliken analysis.

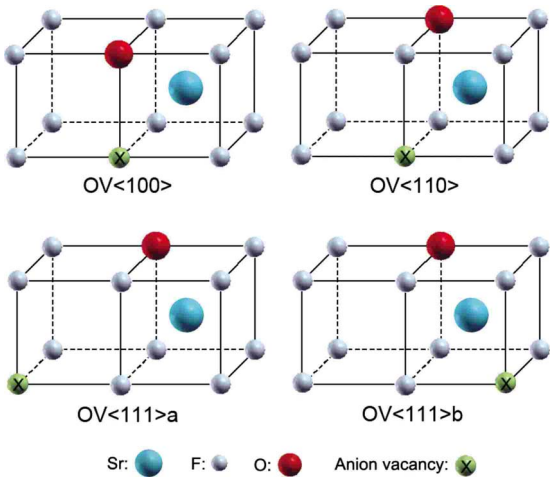

FIG. 1. (Color online) Four different O_V dipole arrangements in an SrF_2 crystal.

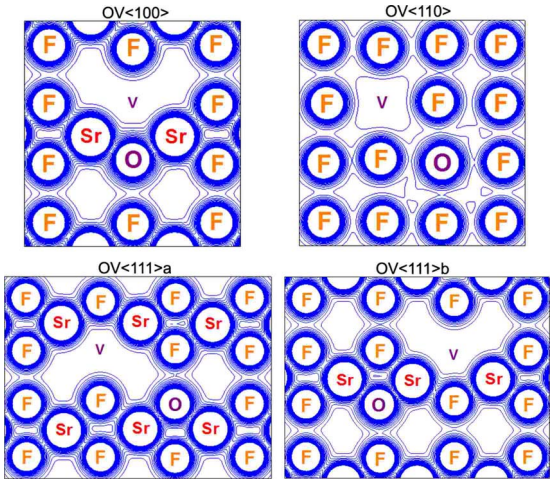

FIG. 2. (Color online) Electron density of the SrF_2 crystal with O_V dipole from 0 to 0.1 e/bohr^3 with an increment of 0.004 e/bohr^3. The $O_V\langle 100\rangle$ diagram and the $O_V\langle 111\rangle a$ diagram refer to the (110) layer. The $O_V\langle 110\rangle$ diagram refers to the (100) layer. The $O_V\langle 111\rangle b$ diagram shows the electron density of the $(1\bar{1}0)$ layer.

III. O_V DIPOLE STRUCTURE IN SrF_2

The O_V dipole is a very important type of point impurity of the SrF_2 crystal. It is made up of an oxygen atom and a vacancy. As shown in Fig. 1, four possibilities of O_V dipole arrangements in the SrF_2 crystal exist. The O_V dipole can be placed on the edge of the cubic crystal structure, as shown in the upper left part of Fig. 1. It is called $O_V\langle 100\rangle$ in the following. Also, the dipole can be placed on a side diagonal of the cube, as shown in the upper right part of Fig. 1. This type of arrangement is called $O_V\langle 110\rangle$. If the dipole is placed in the center of the cube, two types of alignments must be distinguished. One type is shown in the lower left part of Fig. 1. Here, no strontium atom is located between the oxygen atom

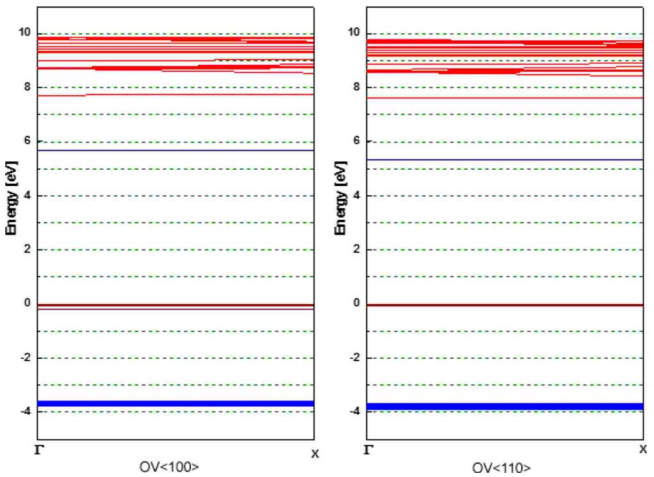

FIG. 3. (Color online) B3PW band structure simulation of two O_V dipole arrangements in a 96-atom supercell of an SrF_2 crystal between −4 and 10 eV. There are three defect bands near the Fermi level and another defect band exists between the Fermi level and conduction band.

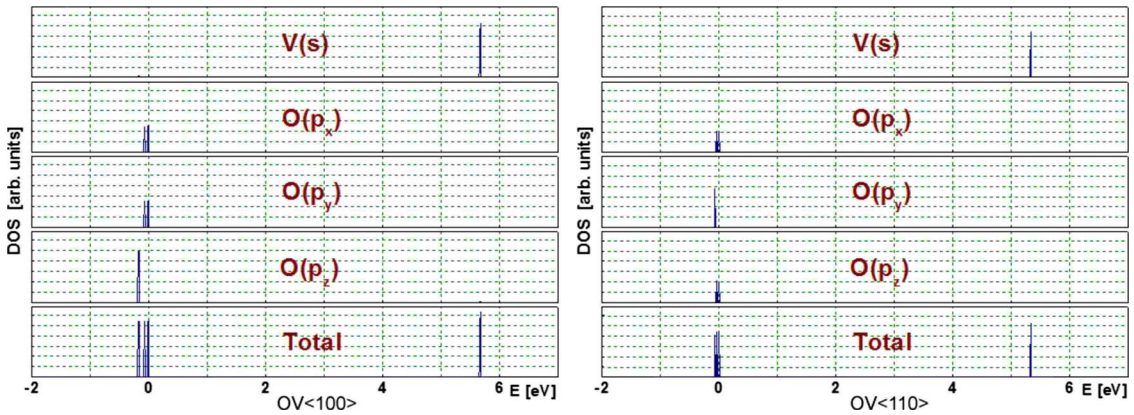

FIG. 4. (Color online) DOS diagram of two O_V dipole arrangements between −2 and 7 eV.

and the vacancy. This type of arrangement is called $O_V\langle 111\rangle a$. If there is a strontium atom located between the oxygen atom and the vacancy, as shown in the lower right part of Fig. 1, we call it $O_V\langle 111\rangle b$. By using Eq. (3) we show the large formation energies of the four O_V dipole impurities in a 96-atom supercell in Table I.

Comparison of the formation energies in Table I allows us to derive the following rule:

$$E_{O_V\langle 100\rangle} < E_{O_V\langle 111\rangle b} < E_{O_V\langle 110\rangle} < E_{O_V\langle 111\rangle a}. \quad (6)$$

The total energy is the lowest if the dipole is arranged in the $O_V\langle 100\rangle$ way. $E_{O_V\langle 100\rangle}$ is 0.20 eV less than $E_{O_V\langle 111\rangle b}$, 0.25 eV less than $E_{O_V\langle 110\rangle}$, and 0.37 eV less than $E_{O_V\langle 111\rangle a}$. Because of the crystal symmetry, $E_{O_V\langle 100\rangle}$ should indeed have the lowest total energy, as well as the total energy of the $O_V\langle 111\rangle$ arrangement should be less than the total energy of the $O_V\langle 110\rangle$ arrangement. It is an unusual result though that $E_{O_V\langle 111\rangle b}$ is 0.17 eV less than $E_{O_V\langle 111\rangle a}$. Likewise, the result indicating that $E_{O_V\langle 111\rangle a}$ is 0.12 eV larger than $E_{O_V\langle 110\rangle}$ is unexpected. This discrepancy probably originates from differences in structure and charge distribution. Due to attractive forces, the existence of a strontium atom at the right side of the plane with the oxygen atom and the vacancy in the upper right part of Fig. 1 decreases the potential difference between oxygen atom and vacancy. Hence, the total energy of the $O_V\langle 111\rangle a$ structure exceeds the total energy of the $O_V\langle 110\rangle$ structure. As mentioned above, all calculations are done in relaxed geometries. The calculated relaxation energies, i.e., the difference of the total energies for the relaxed and unrelaxed atomic configurations, turn out to follow the same sequence as the formation energies: the smallest value (1.59 eV) is obtained for $O_V\langle 100\rangle$ and the largest value (2.48 eV) is obtained for $O_V\langle 111\rangle a$.

IV. ELECTRONIC PROPERTIES OF THE SrF_2 CRYSTAL WITH O_V DIPOLE IMPURITY

The charge distribution in a 96-atom supercell enables us to draw conclusions concerning the total energy and other electronic properties of the SrF_2-O_V system. The charge distribution is of course different for every O_V dipole arrangement. All four situations are shown in Fig. 2. The effective charge of the oxygen atom is −1.700 *e* in the $O_V\langle 100\rangle$ arrangement, −1.738 *e* in the $O_V\langle 110\rangle$ arrangement, −1.737 *e* in the $O_V\langle 111\rangle a$ arrangement, and −1.732 *e* in the $O_V\langle 111\rangle b$ arrangement. The effective charge of the vacancy is close to zero in each case. In detail, it is −0.114 *e* in $O_V\langle 100\rangle$, −0.060 *e* in $O_V\langle 110\rangle$, −0.062 *e* in $O_V\langle 111\rangle a$, and −0.064 *e* in $O_V\langle 111\rangle b$.

The overlap population between the vacancy and the oxygen atom is +102 *me* in the $O_V\langle 100\rangle$ arrangement and thus shows some covalent character. The bond populations between the oxygen atom and neighboring strontium atoms are all negative and below −100 *me*. The negative value indicates a repulsive force. Hence, there are no covalent bonds between the oxygen atom and its neighboring strontium atoms.

To study the optical properties of the SrF_2 crystal with O_V dipoles, the band structures of the four different dipole arrangements are simulated using the B3PW method. The band structures differ only very little near the Fermi level. In the $O_V\langle 100\rangle$ dipole arrangement, which is shown in the left part of Fig. 3, there are three defect bands below the Fermi level and one defect band between the Fermi level and the conduction band. In the $O_V\langle 110\rangle$ dipole arrangement (right plot), the band structure is nearly the same. There are three defect bands close to 0 eV as well, but the differences in energy between the bands are smaller. In the $O_V\langle 111\rangle a$ and $O_V\langle 111\rangle b$ dipole arrangements, the differences between these bands are even less, with the result that the defect bands merge into one nearly degenerated band.

The density of states (DOS) shows that the defect bands close to the Fermi level are all made up solely of the *p*-type

TABLE II. Band gap $\Gamma \rightarrow \Gamma$ of the SrF_2 crystal with four different dipole arrangements in a 96-atom supercell with B3PW method in units of eV.

Band gap	$O_V\langle 100\rangle$	$O_V\langle 110\rangle$	$O_V\langle 111\rangle a$	$O_V\langle 111\rangle b$
$O_1 \rightarrow V$	5.66	5.32	5.14	5.41
$O_2 \rightarrow V$	5.72	5.36	5.15	5.43
$O_3 \rightarrow V$	5.83	5.39	5.15	5.43
$VB \rightarrow V$	9.25	9.00	8.88	9.01
$O_1 \rightarrow CB$	7.72	7.61	7.56	7.72

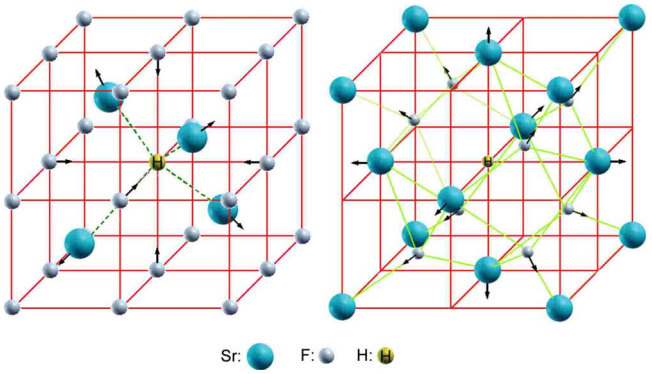

FIG. 5. (Color online) H_s^- and H_i^0 substitution in the SrF_2 crystal structure. Arrows close to neighboring atoms indicate the direction of displacement of these atoms.

orbitals of the oxygen atom in all O_V dipole arrangements. The reason for that are the differences in the potential energy between these four dipole arrangements and between the oxygen atom and the neighboring fluorine atom. As shown in the left plot of Fig. 4, the defect band with the lowest energy in the $O_V\langle 100\rangle$ arrangement is made up solely of the p_z orbitals of the oxygen atom. The two other defect bands are made up of the p_x and p_y orbitals of the oxygen atom together. In the $O_V\langle 110\rangle$ arrangement, as shown in the right plot of Fig. 4, the defect band with the lowest energy is made up solely of the p_y orbitals of the oxygen atom. The other two defect bands are made up of the p_x and p_z orbitals. This coordinate shift is caused by the different orientation of the O_V dipole in each arrangement. In the two other dipole arrangements, there is almost no difference in energy between the three defect bands below the Fermi level. These three bands are called O_3 (lowest energy), O_2 (medium energy), and O_1 (highest energy). The other defect band between Fermi level and conduction band is called V and is made up solely of the exclusive s orbital of the vacancy. In the $O_V\langle 111\rangle b$ arrangement, there is a strontium atom within the O_V dipole. The DOS shows that this atom has nearly no influence on the four defect bands.

TABLE III. Effective charges of atoms in SrF_2 with H_s^- and H_i^0 impurities in a 96-atom supercell. The effective charges are listed in the Q column. "+" indicates cations and "–" indicates anions. ΔQ labels the change in the effective charge compared to a perfect SrF_2 crystal ($Q_{Sr}=+1.909$ e and $Q_F=-0.954$ e). Spin (e) for H_i^0 is the result of the spin difference of electrons with different spin directions ($n_\alpha - n_\beta$).

	With H_s^- impurity			With H_i^0 impurity			
Atom	No. of atoms	Q (e)	ΔQ (e)	No. of atoms	Q (e)	ΔQ (e)	Spin (e)
H	1	−0.962		1	−0.087		0.965
Sr	4	+1.910	+0.001	6	+1.908	−0.001	0.001
F	4[a]	−0.955	−0.001	8[b]	−0.943	+0.011	0.004
	3[c]	−0.955	−0.001				

[a]Fifth neighboring atoms of the H_s^- anion.
[b]First neighboring atoms of the H_i^0 anion
[c]Sixth neighboring atoms of the H_s^- anion.

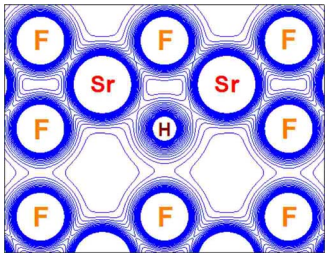

FIG. 6. (Color online) Electron-density diagram of a SrF_2 crystal with H_s^- impurity in a 96-atom supercell in [110] direction. Isodensity curves show densities between 0 and 0.1 e/bohr^3 with an increment of 0.004 e/bohr^3.

The band gaps are listed in Table II. The gaps between the valence and conduction bands are almost not influenced; the value for the perfect crystal being 11.31 eV.[16] The absorption energy is 5.65 eV.[25] This energy is almost identical with the calculated band gap $O_1 \rightarrow V$ in the $O_V\langle 100\rangle$ arrangement, which is 5.66 eV. A comparison of these band gaps $O_1 \rightarrow V$ of all four O_V dipole arrangements points out that the values are in opposite order of the total energy rule (6) of a SrF_2 crystal with O_V dipoles in a 96-atom supercell. It shows from another viewpoint once more that the $O_V\langle 100\rangle$ arrangement is more stable than the others.

V. CALCULATION OF THE H_s^- IMPURITY IN SrF_2

Now we want to focus on the so-called H_s^- impurity of the SrF_2 crystal. As shown in the left plot of Fig. 5, a fluorine anion is substituted by a H^- ion in this process. The formation energy is shown in Table I and is more than 1 order of magnitude smaller than that for the O_V dipole impurities. The relaxation energy (0.008 eV) is nearly negligible. The arrows close to neighboring atoms of the H_s^- anion indicate the direction of displacement of these atoms. The first neighboring atoms, four strontium atoms, move away from the H_s^- anion

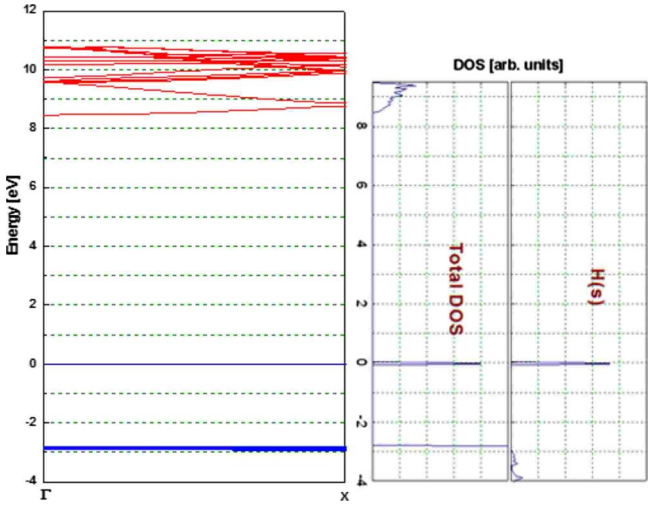

FIG. 7. (Color online) Band structure and DOS diagrams of a SrF_2 crystal with H_s^- impurities in a 96-atom supercell. There is only one defect band just below the Fermi level.

TABLE IV. Band gap $\Gamma \rightarrow \Gamma$ (eV) of a SrF_2 crystal with H_s^- impurity.

Band gap	Our results	Expt. results[a]	Theor results[b]	Theor results[c]
$H_s^- \rightarrow$ CB	8.47	7.04	5.90	6.37
VB $\rightarrow H_s^-$	2.81			

[a]Reference 27.
[b]Reference 28.
[c]Reference 29.

by 0.02% in terms of the lattice constant $a_0=5.845$ Å.[16] This movement equals in its absolute value the corresponding H_s^- movement in BaF_2 but has the opposite sign.[26] The second neighboring atoms, six fluorine atoms, get closer to the H_s^- ion by 0.08% in terms of the lattice constant. This result corresponds to simulations of the H_s^- substitution in BaF_2 and CaF_2.[26] All the distance changes (or relaxations) between the H_s^- anion and its neighboring atoms are relatively small. Therefore the changes in the effective charges of the neighboring atoms should only be small. This is confirmed by the data in Table III. The hydrogen atom taking over the position of a fluorine anion exhibits an effective charge only 8 *me* less than the effective charge of a fluorine anion in the perfect SrF_2 crystal. The effective charge of the first neighboring atoms (four strontium atoms) has increased by 1 *me*, while the effective charge of the fifth and sixth neighboring atoms (four and three fluorine atoms) has decreased by 1 *me*. The effective charges of all other atoms remain the same as in a perfect SrF_2 crystal.

Figure 6 shows the electron distribution of the (110) surface. The isodensity curves drawn in this diagram range from 0 to 0.1 e/bohr^3 with an increment of 0.004 e/bohr^3. These curves visualize the electron distribution change close to the substituting hydrogen atom.

The band structure of a SrF_2 crystal with H_s^- impurities is shown in Fig. 7. The figure shows an additional straight line in addition to the band structure of a perfect SrF_2 crystal.

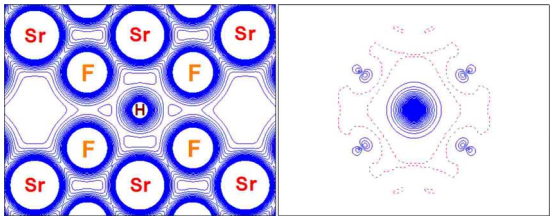

FIG. 8. (Color online) Left plot: Electron-density diagram of a SrF_2 crystal with H_i^0 impurity between 0 and 0.1 e/bohr^3 with an increment of 0.004 e/bohr^3. Right plot: Spin-density diagram of a SrF_2 crystal with H_i^0 impurity between −0.5 and 0.3 e/bohr^3 with an increment of 0.005 e/bohr^3 where the short dotted lines indicate null isodensity lines and solid lines indicate the positive ones. Both diagrams show the electron distribution of the (110) surface.

Examination of the DOS (see the right plot of Fig. 7) points out that this band consists of *s* orbitals from the substituting hydrogen atom only. Calculations show that this defect band is very narrow with a bandwidth of only 0.01 eV.

The calculated band gaps are listed in Table IV. The gap between conduction and defect bands at the Γ point is calculated to be 8.47 eV. The corresponding energy difference between the top of the valence band and the defect band is found to be 2.81 eV. Compared to the results published by Shi,[26] our results lie in between the energy differences of the corresponding bands in BaF_2 and CaF_2. The transition energy of SrF_2 with H_s^- was determined experimentally to be 7.04 eV.[27] For comparison, two other theoretical results[28,29] are listed in Table IV as well.

VI. CALCULATION OF THE H_i^0 IMPURITY IN SrF_2

Another interesting kind of hydrogen impurity is the H_i^0 impurity shown in the right plot of Fig. 5. The hydrogen atom is inserted into the center of the crystal without substituting another atom. The formation energy of the H_i^0 impurity is extremely low, only 0.07 eV (shown in Table I). The

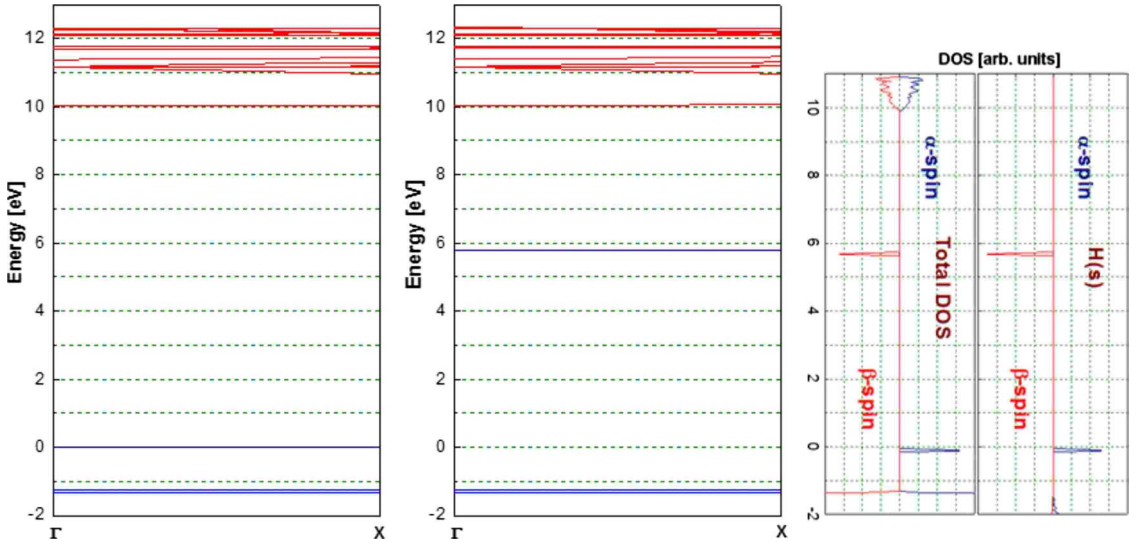

FIG. 9. (Color online) α-defect (left) and β-defect (right) band structures and corresponding DOS diagram of a SrF_2 crystal with H_i^0 impurity, calculated in a 96-atom supercell.

TABLE V. Band gap $\Gamma \rightarrow \Gamma$ (eV) of a SrF_2 crystal with H_i^0 impurity.

Band gap	α	β
$H_i^0 \rightarrow CB$	10.03	4.24
$VB \rightarrow H_i^0$	1.23	7.04

relaxation energy is even below 1 meV. The arrows once again indicate the direction of relaxation of the labeled atoms. In this case, all neighboring atoms move away from the hydrogen impurity. The first neighbors are eight fluorine atoms. They increase their distance to the impurity by 0.19% in terms of the lattice constant. The second neighbors, six strontium atoms, relax by only 0.006% in terms of the lattice constant.

The electron distribution data in Table III show that the effective charge of the hydrogen impurity is negative and very small ($-0.087\ e$). The effective charge of the first neighboring atoms, however, shows a remarkably large increase in effective charge, about 11 *me*. The charge of the second neighboring atoms is decreased by 1 *me* only. Since in the H_i^0 impurity system there is an unpaired electron, such as in a F-center system, it will be strongly polarized. The spin charge of the hydrogen atom is almost 1 *e*, while that of all other atoms remains almost zero [spin(F)=4 *me*, spin(Sr)=1 *me*]. Figure 8 shows the electron distribution and the spin-density diagram in the right plot. The short dotted lines indicate the null isodensity lines. The electron-spin density around H_i^0 is very large. Spin polarization cannot be found close to strontium atoms but close to the fluorine atoms. However, this spin polarization has only a very weak effect on the other atoms.

Because of the strong spin polarization of the H_i^0 impurity, there exist two defect bands with different spin polarizations at quite different energies. The DOS shows that the lower defect band close to 0 eV is made up of *s*-type orbitals from the hydrogen impurity with α spin (spin up), while the higher-energy defect band is made up of *s*-type orbitals with β spin (spin down). Only the α-spin defect band is occupied. Electron transition from the occupied α-defect band to the unoccupied β-defect band is not allowed because of spin selection rules (Fig. 9). Hence Table V does not include the energy gap between the two defect bands. The band gap between α defect and conduction bands is 10.03 eV.

Since there is one electron in the system that cannot be paired with other electrons, the spin of this electron interacts with the nuclear spin of the nearby nuclei. Hence the electron paramagnetic resonance (EPR) spectrum of this electron can be used to find the hyperfine structure of the system with H_i^0 impurity and the associated hyperfine constants. In case of the hydrogen (deuterium) site only the isotropic coupling component (a) may be nonzero. The corresponding calculated and experimentally derived hyperfine constants plus those at the nearest-neighbor eight fluorine atoms are listed in Table VI. Our calculated results are close to the experimental ones. Results for the second-nearest neighbors (six strontium atoms) are almost zero.

TABLE VI. Experimentally and theoretically determined hyperfine constants a and b (in MHz) at the hydrogen atom (^{1}H), deuterium atom (^{2}H), and at its eight nearest fluorine neighbors in the H_i^0 system.

	Our results		Expt. results[a]		Theor results	
	a	b	a	b	a	b
^{1}H	1358.0	0	1444.16		1403[b]	
^{2}H	208.45	0				
F	66.34	28.44	70.76	28.19	31[c]	

[a]Reference 30.
[b]Reference 1.
[c]Reference 31.

VII. CONCLUSION

The present work presents calculations for four different O_V dipole structures and their electronic properties in SrF_2 systems calculated by the hybrid B3PW method with a quite simple basis set for the fluorine vacancy. The lowest total energy of the SrF_2 system with $O_V\langle 100\rangle$ impurity represents the most stable arrangement of oxygen-vacancy dipoles in a SrF_2 crystal. Because of the very low formation energy the H_i^0 impurity can be most easily produced. The defect bands below the Fermi level are made up of the *p* orbitals of the oxygen atom in every O_V dipole arrangement. The other defect band above the Fermi level is made up of the *s* orbital of the vacancy. In the second part of this work we present also corresponding results for hydrogen impurities. There are two different types of hydrogen impurities called H_s^- and H_i^0. The calculated properties of H_s^- and H_i^0 impurities agree well with experimental data and are found better than in former theoretical results.

*Also at Department of Mathematics and Natural Sciences, Bergische Universität Wuppertal, D-42097 Wuppertal, Germany; rajia@uni-wuppertal.de.
†Also at Department of Physics and Materials Science, Uppsala University, SE-75121 Uppsala, Sweden.

[1] W. Hayes, *Crystals with the Fluorite Structure* (Clarendon, Oxford, 1974).
[2] C. S. Yoo, H. B. Radousky, N. C. Holmes, and N. M. Edelstein, Phys. Rev. B **44**, 830 (1991).
[3] J. J. Tu and A. J. Sievers, Phys. Rev. Lett. **83**, 4077 (1999).
[4] K. Inoue, N. Suzuki, and T. Hyodo, Phys. Rev. B **71**, 134305 (2005).
[5] T. Kohmoto, Y. Fukuda, M. Kunitomo, and K. Isoda, Phys. Rev. B **62**, 579 (2000).
[6] J. M. Vail, W. A. Coish, H. He, and A. Yang, Phys. Rev. B **66**, 014109 (2002).

[7] J. A. Weil, J. R. Bolton, and J. E. Wertz, *Electron Paramagnetic Resonance* (Wiley, New York, 1994).
[8] D. R. Lide, *Handbook of Chemistry and Physics* (CRC, Boston, 1991).
[9] Axel D. Becke, J. Chem. Phys. **98**, 5648 (1993).
[10] J. P. Perdew and Y. Wang, Phys. Rev. B **33**, 8800 (1986).
[11] J. P. Perdew and Y. Wang, Phys. Rev. B **40**, 3399 (1989).
[12] J. P. Perdew and Y. Wang, Phys. Rev. B **45**, 13244 (1992).
[13] H. Shi, R. I. Eglitis, and G. Borstel, Phys. Rev. B **72**, 045109 (2005).
[14] H. Shi, R. I. Eglitis, and G. Borstel, J. Phys.: Condens. Matter **18**, 8367 (2006).
[15] R. I. Eglitis, H. Shi, and G. Borstel, Surf. Rev. Lett. **13**, 149 (2006).
[16] R. Jia, H. Shi, and G. Borstel, Comput. Mater. Sci. **43**, 980 (2008).
[17] R. Dovesi, V. R. Saunders, C. Roetti, R. Orlando, C. M. Zicovich-Wilson, F. Pascale, B. Civalleri, K. Doll, N. M. Harrison, I. J. Bush, Ph. D'Arco, and M. Llunell, *CRYSTAL06 User's Manual* (University of Torino, Italy, 2008).
[18] V. R. Saunders, Faraday Symp. Chem. Soc. **19**, 79 (1984).
[19] M. P. Habas, R. Dovesi, and A. Lichanot, J. Phys.: Condens. Matter **10**, 6897 (1998).
[20] R. Nada, C. R. A. Catlow, C. Pisani, and R. Orlando, Modell. Simul. Mater. Sci. Eng. **1**, 165 (1993).
[21] L. Valenzano, F. J. Torres, K. Doll, F. Pascale, C. M. Zicovich-Wilson, and R. Dovesi, Z. Phys. Chem. **220**, 893 (2006).
[22] G. Mallia, R. Orlando, C. Roetti, P. Ugliengo, and R. Dovesi, Phys. Rev. B **63**, 235102 (2001).
[23] R. Dovesi, C. Ermondi, E. Ferrero, C. Pisani, and C. Roetti, Phys. Rev. B **29**, 3591 (1984).
[24] H. J. Monkhorst and J. D. Pack, Phys. Rev. B **13**, 5188 (1976).
[25] E. Radzhabov, J. Phys.: Condens. Matter **6**, 9807 (1994).
[26] H. Shi, R. I. Eglitis, and G. Borstel, J. Phys.: Condens. Matter **19**, 056007 (2007).
[27] J. H. Beaumont, W. Hayes, D. L. Kirk, and G. P. Summers, Proc. R. Soc. London, Ser. A **315**, 69 (1970).
[28] R. S. Singh, D. W. Galipeau, and S. S. Mitra, J. Chem. Phys. **52**, 2341 (1970).
[29] H. S. Bennett, Phys. Rev. B **6**, 3936 (1972).
[30] R. G. Bessent, W. Hayes, J. W. Hodby, and P. H. S. Smith, Proc. R. Soc. London, Ser. A **309**, 69 (1969).
[31] R. G. Bessent, W. Hayes, and J. W. Hodby, Proc. R. Soc. London, Ser. A **297**, 376 (1967).